Journal of Coupled Systems and Multiscale Dynamics

doi:10.1166/jcsmd.2014.1038
J. Coupled Syst. Multiscale Dyn.
Vol. 2(1)/2330-152X/2014/001/008

Transport efficiency of the human placenta

Qinglan Xia[1,*] and Carolyn Salafia[2]

[1]*Department of Mathematics, University of California at Davis, Davis, CA, 95616*
[2]*Placental Analytics, LLC, Larchmont NY 10538. Institute for Basic Research, Staten Island, NY*

(Received: 14 May 2014. Accepted: 13 June 2014)

ABSTRACT

The human newborn is a reflection of the entirety of nutrients transferred from the maternal to the fetal circulation across the placenta during gestation. By extension, birth weight and newborn health depend on placental function. In this article, we quantify efficiency of the transport system in the human placenta and study its role played in the birth weight as well as the gestational age of the human newborn. In the data, each placenta is represented by a planar domain and a fixed point representing the site of the umbilical cord insertion. By means of techniques in ramified optimal transportation, we simulate a vascular tree structure for the placenta, in a simplified form by an idealized optimal transport network. We study transport efficiency of this simulated transport network for each placenta and investigate its correlations with birth weight and gestational age at birth. We show that averaged birth weight and averaged gestational age are both roughly increasing functions of the calculated placental transport efficiency. Both preterm and low birth weight are associated with lower placental transport efficiency. We also show that the relationship of transport efficiency to these outcomes is nonlinear, reaching a plateau at 38–39 weeks gestational age and 3200 g birth weight.

Keywords: Placenta, Birth Weight, Optimal Transportation, Transport Efficiency, Shape Factor, Branching Structure.

Section: Life, Climate & Environmental Sciences

Research Article

1. INTRODUCTION

The human newborn is the reflection of the sum total of oxygen and nutrients transferred from the maternal to the fetal circulation across the placenta during gestation. By extension, efficiency of the transport system in the placenta plays an important role in determining the birth weight, the placental weight and the gestational age of the newborn. The goal of this paper is to apply optimal transport modeling to quantify effects of efficiency of the transport system in human placentas on the birth weight as well as the gestational age. For each placenta, we simulate a vascular tree structure in a simplified form by an idealized optimal transport network. The simulation of the vascular tree structure is based on (i) placental size, (ii) placental shape and (iii) the position of insertion of the umbilical cord on the chorionic disk surface. This size, shape and position data was readily available from measurements from photographs of 1110 placentas from a University of North Carolina birth cohort collected in the middle of the last decade, which has been extensively studied in e.g., Refs. [3, 6, 7, 16, 20] and references therein. For each simulated transport network, there is an associated transport cost C, computed by the model. This cost C represents the total work done by the heart of fetus to pump blood across the placenta. We find a high correlation between C and measured birth weight. Averaged transport cost is nearly a linear function of the birth weight. Also, a shape factor S is computed by the model which would be the transport cost if a placenta were rescaled to have a unit area chorionic plate. The shape factor is the same for two placentas of the same shape. Moreover, we define transport efficiency

*Author to whom correspondence should be addressed.
Email: qlxia@math.ucdavis.edu

E of the placenta to be the ratio of the corresponding shape factor (i.e., normalized transport cost) of the unit disk with the one of the placenta. We show that averaged birth weight and averaged gestational age are both roughly increasing functions of the calculated placental transport efficiency. Both preterm and low birth weight are associated with lower placental transport efficiency. We also show that the relationship of transport efficiency to these outcomes is nonlinear, reaching a plateau at 38–39 weeks gestational age and 3200 g birth weight.

We organize this paper as follows. After recalling some basic concepts about ramified optimal transportation in Section 2, we simulate a vascular structure for each placenta in Section 3 using optimal transport modeling. Via the corresponding transport cost of the vascular structure, we introduce our main concepts: the shape factor and the transport efficiency, for each placenta. In the last section, we investigate the relations of the calculated transport cost and placental transport efficiency with the measured birth weight as well as the gestational age at birth.

Some Related Works on Human Placentas. The first related approach is given in Ref. [15] where a 3D one-parameter model of placental vascular growth is proposed based on diffusion limited aggregation. Another approach is given in Ref. [3] using the diffusion method. By considering villous membrane to capillary membrane transport, stationary oxygen diffusion can be numerically solved in terminal villi represented by digital photomicrographs. We refer to Ref. [19] and references therein for the updated research in this direction. The third interesting approach is given in Ref. [17] which investigated thermodynamic properties of optimal transport networks while[18] investigates thermodynamic properties of measured human placenta major blood vessel networks.

2. BRIEF INTRODUCTION TO RAMIFIED OPTIMAL TRANSPORTATION

The optimal transportation problem aims at finding an optimal way to transport materials from the source to the target. An optimal transport path introduced in Ref. [9] is a mathematical concept used to model tree-shaped branching transport networks. Transport networks with branching structures are observable not only in nature as in trees, blood vessels, river channel networks, lightning, etc. but also in efficiently designed transport systems such as used in railway configurations and postage delivery networks. Recently, mathematicians (e.g., Refs. [1, 2, 4, 9]) have shown great interest in modeling these transport networks with branching structures. Applications of optimal transport paths may be found in e.g., Refs. [10 and 13]. In this article, we will model the blood vessel structure of a placenta via an optimal transport path.

We first recall some basic concepts of ramified optimal transportation as stated in Ref. [9]. Recall that a (finite) atomic measure on the Euclidean space $\mathbb{R}^m$ is in the form of

$$\mathbf{a} = \sum_{i=1}^{k} m_i \delta_{x_i} \tag{1}$$

with distinct points $x_i \in \mathbb{R}^m$, and positive real numbers m_i, where δ_x denotes the Dirac mass located at the point x.

Given two atomic measures

$$\mathbf{a} = \sum_{i=1}^{k} m_i \delta_{x_i} \quad \text{and} \quad \mathbf{b} = \sum_{j=1}^{\ell} n_j \delta_{y_j} \tag{2}$$

in $\mathbb{R}^m$ of equal mass (i.e., $\sum_{i=1}^{k} m_i = \sum_{j=1}^{\ell} n_j$), a *transport path* from $\mathbf{a}$ to $\mathbf{b}$ is a weighted directed graph G consisting of a vertex set $V(G)$, a directed edge set $E(G)$ and a weight function w: $E(G) \to (0, +\infty)$ such that $\{x_1, x_2, \ldots, x_k\} \cup \{y_1, y_2, \ldots, y_\ell\} \subset V(G)$ and for any vertex $v \in V(G)$,

$$\sum_{e \in E(G),\, e^- = v} w(e) - \sum_{e \in E(G),\, e^+ = v} w(e) = \begin{cases} m_i, & \text{if } v = x_i \text{ for some } i = 1, \ldots, k \\ -n_j, & \text{if } v = y_j \text{ for some } j = 1, \ldots, \ell \\ 0, & \text{otherwise} \end{cases}$$

where e^- and e^+ denotes the starting and ending endpoints of each edge $e \in E(G)$.

Note that this balanced equation simply means the conservation of mass at each vertex.

Suppose $\mathbf{a}$ and $\mathbf{b}$ are two atomic measures on $\mathbb{R}^m$ of equal total mass. For any real number $\alpha < 1$ and any transport path G from $\mathbf{a}$ to $\mathbf{b}$, we define its *transport cost* to be

$$\mathbf{M}_\alpha(G) := \sum_{e \in E(G)} w(e)^\alpha \mathit{length}(e) \tag{3}$$

where $\mathit{length}(e)$ denotes the Euclidean distance between endpoints of the edge e.

Let $\mathit{Path}(a, b)$ be the space of all transport paths from $\mathbf{a}$ to $\mathbf{b}$. A transport path G from $\mathbf{a}$ to $\mathbf{b}$ is called an *α-optimal transport path* if

$$\mathbf{M}_\alpha(G) \le \mathbf{M}_\alpha(\tilde{G})$$

for any other transport path $\tilde{G}$ from $\mathbf{a}$ to $\mathbf{b}$. Also, the d_α distance between $\mathbf{a}$ and $\mathbf{b}$ is defined to be

$$d_\alpha(\mathbf{a}, \mathbf{b}) = \min\{\mathbf{M}_\alpha(G) \colon G \in \mathit{Path}(\mathbf{a}, \mathbf{b})\} \tag{4}$$

In general, for any two Radon measures μ and ν on $\mathbb{R}^m$ with equal mass, the d_α distance between μ and ν is given by

$$d_\alpha(\mu, \nu) = \lim_{n \to \infty} d_\alpha(\mathbf{a}_n, \mathbf{b}_n) \tag{5}$$

for any two sequence $\{\mathbf{a}_n\}, \{\mathbf{b}_n\}$ of atomic measures converge weakly to μ and ν, respectively.

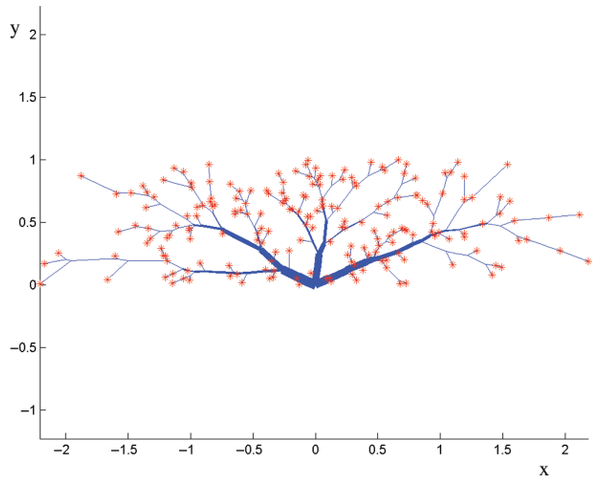

Fig. 1. An optimal transport path from 100 random points to the origin.

Some numerical simulations of optimal transport paths were given in Ref. [12]. For instance, Figure 1 provides a typical example of an optimal transport path.

Applications of optimal transport path may be found in e.g., Refs. [10, 13 and 11]. For instance, we have used the idea of theory to understand the dynamic formation of a plant leaf in Ref. [10].

3. THE SHAPE FACTOR AND TRANSPORT EFFICIENCY OF A PLACENTA

As stated in Ref. [16], 1110 placentas were collected by an academic health center in central North Carolina. For each placenta, a trained observer captured series of x, y coordinates that marked the site of the umbilical cord insertion and the perimeter of the fetal surface. To simulate vascular structures for the placentas, we apply the modeling method of ramified optimal transportation to each placenta.

The vascular network structure in each placenta provides a means of transporting blood between the whole chorionic plate surface and the umbilical cord. In a simplified version, this network may be represented by a weighted directed graph. For each branch point of this network, the sum of flows in must equal the sum of flows out. This motives us to view it as a transport path from the chorionic plate to the umbilical cord. Since there are many ways to construct a transport network one would like to find an optimal one which minimizes the amount of work done to pump the blood. The transportation cost for each transport path reflects the work done in pumping blood through the network. As a result, we use an optimal transport path to simulate an optimal vascular structure for that placenta. This single idealized network for a placenta may be viewed as a representation of either an optimal vein network or, by reversing directions of flow, an optimal arterial network. In the absence of more detailed information about blood supply, we assume a uniform supply of blood per unit area over the whole surface of the placenta. We also model the placenta by a region in the plane because the data is from photographs of the placenta flat on a table, rather than in the curved inside surface of the uterus.

3.1. The Shape Factor and the Transport Efficiency

As stated above, each placenta P is represented by a pair (D, O) where D is a bounded planar domain and O is a fixed point inside D representing the the site of the umbilical cord insertion. Let μ_D denote the Lebesgue measure of $\mathbb{R}^2$ restricted on the set D. For each $\alpha < 1$, the transport cost of the placenta $P = (D, O)$ is defined to be

$$C_\alpha(P) := d_\alpha(\mu_D, |D|\delta_O)$$

where $|D|$ denotes the area of the domain D. By properties of d_α, it holds that

$$C_\alpha(P) = |D|^\alpha d_\alpha\left(\frac{1}{|D|}\mu_D, \delta_O\right)$$

Let $P_1 = (D_1, O_1)$ and $P_2 = (D_2, O_2)$ be two placentas. We say P_1 and P_2 have the same shape if there exists a number $\lambda > 0$ such that the mapping f_λ: $D_1 \to D_2$ given by

$$f(x) = \lambda(x - O_1) + O_2, x \in D_1$$

is one-to-one and onto. The number λ is called the rescale factor.

We are interested in investigating the role of the shape of the placenta played in the birth weight of the newborn. Thus, we introduce the variable "shape factor" as follows.

DEFINITION 3.1. *For each placenta $P = (D, O)$ and $\alpha < 1$, the α-shape factor of P is defined by*

$$S_\alpha(P) := \frac{\mathbf{C}_\alpha(P)}{|D|^{\alpha+0.5}} = \frac{d_\alpha((1/|D|)\mu_D, \delta_O)}{\sqrt{|D|}}$$

PROPOSITION 3.2. *Let $P_1 = (D_1, O_1)$ and $P_2 = (D_2, O_2)$ be two placentas. If P_1 and P_2 have the same shape, then they have the same shape factor. That is,*

$$S_\alpha(P_1) = S_\alpha(P_2)$$

for each α,

PROOF. Since D_2 is a rescale of D_1 in $\mathbb{R}^2$, it holds that

$$|D_2| = \lambda^2|D_1|$$

By the definition of the transport cost $\mathbf{M}_\alpha$, one may also show that

$$d_\alpha\left(\frac{1}{|D_2|}\mu_{D_2}, \delta_{O_2}\right) = \lambda d_\alpha\left(\frac{1}{|D_1|}\mu_{D_1}, \delta_{O_1}\right)$$

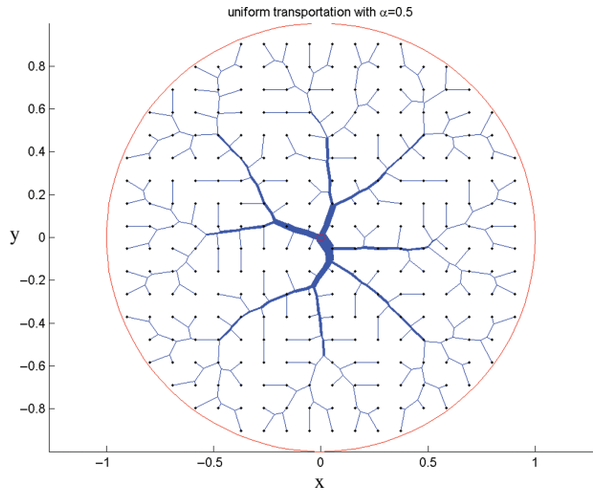

Fig. 2. An approximated 0.5-optimal transport path.

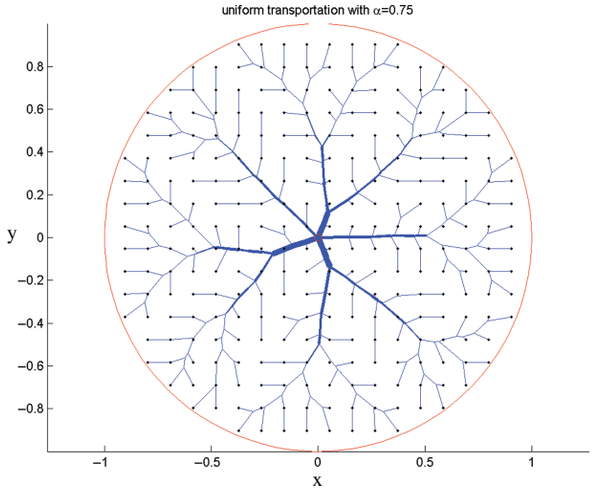

Fig. 4. An approximated 0.75-optimal transport path.

Therefore,

$$S_\alpha(P_2) = \frac{d_\alpha((1/|D_2|)\mu_{D_2}, \delta_{O_2})}{\sqrt{|D_2|}} = \frac{\lambda d_\alpha((1/|D_1|)\mu_{D_1}, \delta_{O_1})}{\sqrt{\lambda^2|D_1|}}$$
$$= \frac{d_\alpha((1/|D_1|)\mu_{D_1}, \delta_{O_1})}{\sqrt{|D_1|}} = S_\alpha(P_1)$$

Since transportation cost $d_\alpha((1/|D|)\mu_D, \delta_O)$ is proportional to the shape-factor S_α, among placentas of similar sizes, the small the shape-factor S_α the more efficient was the transport system corresponding to the placenta. This motivates us to consider the following definition:

DEFINITION 3.3. For each placenta $P = (D, O)$ and $\alpha < 1$, the transport α-efficiency of P is defined to be

$$E_\alpha(P) := \frac{S_\alpha(B(0,1))}{S_\alpha(P)}$$

where $S_\alpha(B(0,1))$ denotes the α-shape factor of the unit ball $B(0,1)$ in $\mathbb{R}^2$ with respect to the origin 0.

Clearly, two placentas of the same shape have the same transport efficiency.

3.2. Vessel Structure Modeled by an Optimal Transport Path

To calculate the transport cost $C_\alpha(P)$, the shape factor $S_\alpha(P)$ and the transport efficiency $E_\alpha(P)$ of a placenta P, we need both the area $|D|$ and the distance $d_\alpha((1/|D|)\mu_D, \delta_O)$. By (5), $d_\alpha((1/|D|)\mu_D, \delta_O)$ is the limit of $d_\alpha(\mathbf{a}_n, \delta_O)$ for any sequence of atomic probability measures $\{\mathbf{a}_n\}$ that is weakly convergent to $(1/|D|)\mu_D$ as probability measures. Here, the value $d_\alpha((1/|D|)\mu_D, \delta_O)$ is independent of the choices of the approximating measures $\{\mathbf{a}_n\}$.

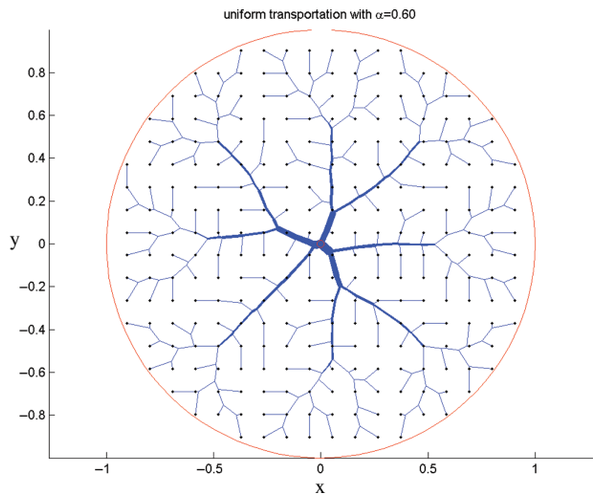

Fig. 3. An approximated 0.6-optimal transport path.

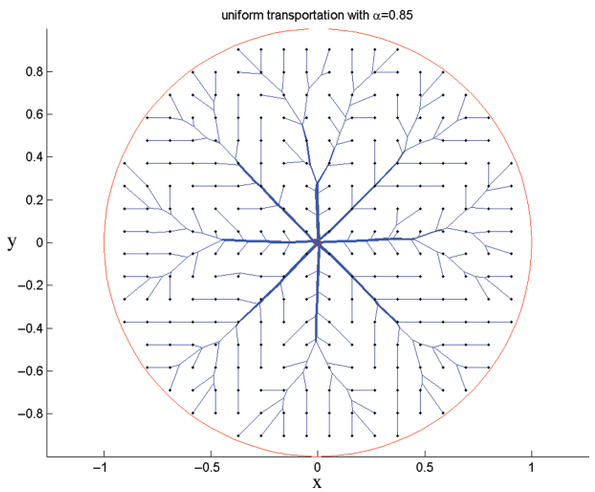

Fig. 5. An approximated 0.85-optimal transport path.

Let $|D|$ be the area of the planar domain D. For each $N \in \mathbb{N}$, let Γ_N be the grid with edge length $h = \sqrt{|D|/N}$ such that the point O is one of the grid points on Γ_N. We approximate the normalized Lebesgue measure $1/(|D|)\mu_D$ by the atomic probability measure

$$\mathbf{a_N} = \frac{1}{\tilde{N}} \sum_{i=1}^{\tilde{N}} \delta_{x_i}$$

where $\{x_1, x_2, \ldots, x_{\tilde{N}}\}$ denote the locations of grid points on Γ_N within the domain D. Note that $\tilde{N} \approx N$ when N is large enough. Also, the sequence $\{\mathbf{a}_N\}$ weakly converges to $(1/|D|)\mu_D$ as $N \to \infty$. As a result, when N is large enough, the transport cost

$$\mathbf{C}_\alpha(P) = |D|^\alpha d_\alpha\left(\frac{1}{|D|}\mu_D, \delta_O\right) \approx |D|^\alpha d_\alpha(\mathbf{a}, \delta_O)$$

and the shape factor

$$S_\alpha(P) = \frac{\mathbf{C}_\alpha(P)}{|D|^{\alpha+0.5}} \approx \frac{d_\alpha(\mathbf{a}, \delta_O)}{\sqrt{|D|}}$$

By definition, the distance $d_\alpha(\mathbf{a}, \delta_O)$ equals to the transport cost $\mathbf{M}_\alpha(G)$ for any optimal transport path $G \in Path(\mathbf{a}, \delta_O)$. When N is small (e.g., less than 20), an optimal transport path G can be found using Melzak's method.[1] When N is large, one can find an approximate optimal transport path G using methods illustrated in Ref. [12]. In our calculations, we take $N = 400$.

Figures 2–5 illustrate some approximated optimal transport paths from the Lebesgue measure on the unit ball $B(0, 1)$ to the Dirac mass $\delta_{(0,0)}$ at the origin under various values of parameter $\alpha < 1$.

Ramark 3.4. Here, we assume $\mathbf{a}$ is uniformly distributed on grid points in the unit ball. Instead, one may also assume $\mathbf{a}$ is randomly distributed in the unit balls. In this case, approximated α-optimal transport paths look like the figures shown in Figures 6 and 7.

Since the values corresponding to randomly distributed masses may vary for each calculation, for simplicity, we still assume the support of $\mathbf{a}$ is uniformly distributed in our calculation.

As a result, for any $\alpha < 1$, one can find approximate values $C_\alpha(P)$, $S_\alpha(P)$ and $E_\alpha(P)$ for any placenta $P = (D, O)$. In practice we picked $\alpha = 0.85$ to give the rate of branching that would give 6 vessels coming from the umbilical cord when the placenta is a typical placenta as illustrated by Figure 8.

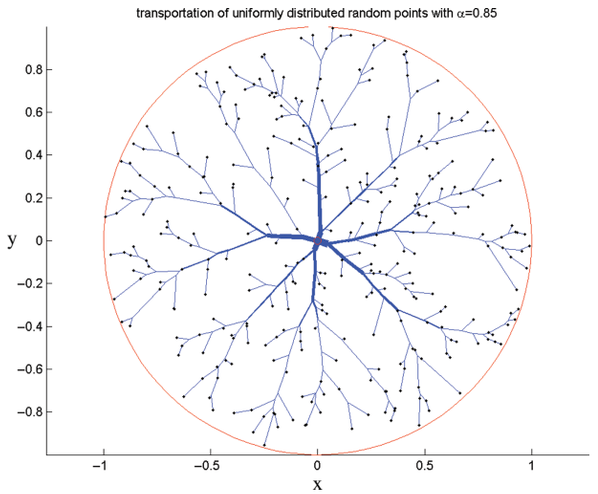

Fig. 7. An approximated 0.85-optimal transport path from randomly distributed points in the unit ball to the origin.

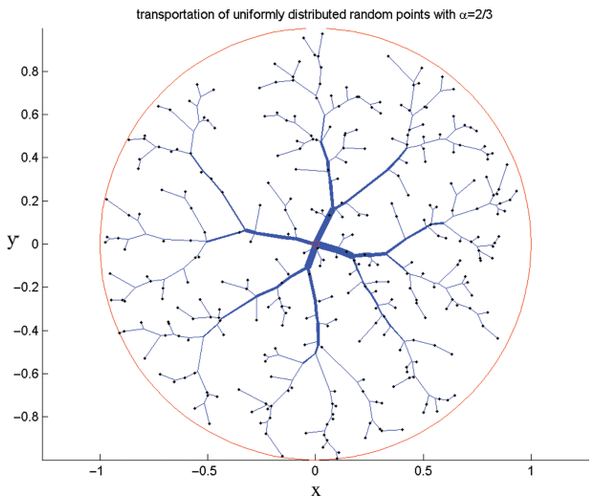

Fig. 6. An approximated 2/3-optimal transport path from randomly distributed points in the unit ball to the origin.

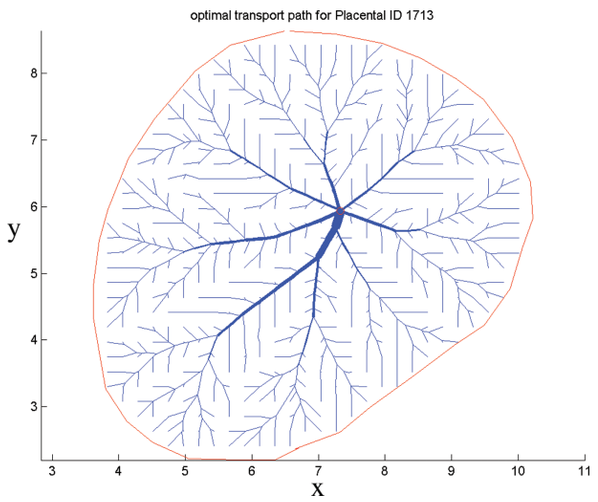

Fig. 8. An example of modeling blood vessels of a placenta by an optimal transport path.

4. RESULTS

For each placenta P in the available data and $\alpha = 0.85$, we calculate the transport cost $C_\alpha(P)$, shape-factor $S_\alpha(P)$ as well as the transport efficiency $E_\alpha(P)$.

4.1. Transport Cost versus Birth Weight

Figure 9 illustrates that the average of transport cost C_α is nearly a linear function of birth weight. Here, for each birth weight B in $\{500, 1000, \ldots, 5000\}$ grams, we calculate the average of transport costs of placentas whose birth weights are among $(B-500, B+500)$ grams. Transport cost C is positively correlated with birth weight as expected given that C primarily reflects placental size, and on average will vary with larger and smaller placental and fetal weights.

4.2. Transport Efficiency versus Birth Weight

We also investigate the relationship between average transport efficiency and birth weights. Again, for each birth weight B in $\{500, 1000, \ldots, 5000\}$ grams, we calculate the average of transport efficiency of placentas whose birth weights are among $(B-500, B+500)$ grams. Figure 10 indicates that averaged transport efficiency is roughly an increasing function of birth weights. The small the birth weight, the less efficient was the placenta. This demonstrates that transport efficiency of the placenta has an important role in the eventual birth weight. By contrast, in Ref. [16], the authors found a 0.75 power relationship between birth weight and placental weight, not efficiency.

Figure 11 indicates that the contribution of placental transport efficiency to the eventual birth weight plateaus above a certain level of transport efficiency. In Figure 11, for each fixed transport efficiency E in $\{0.3, 0.4, \ldots, 1.2\}$, we calculate the mean birth weight of newborns whose placentas have transport efficiency in the range of $(E-0.2, E+0.2)$. Average birth weight still increases as transport efficiency increases, but with a decreased slop, indicating a smaller effect.

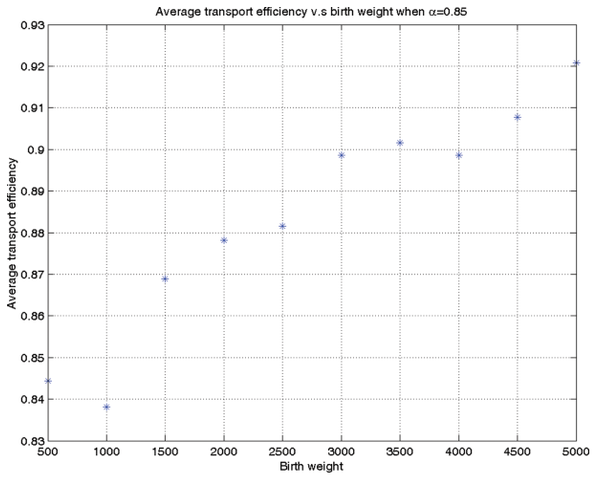

Fig. 10. Average transport efficiency is roughly an increasing function of birth weights.

4.3. Transport Efficiency versus Gestational Age

Finally, we investigate the relationship between average transport efficiency and gestational age. For each gestational age W in [35, 42] weeks, we calculate the average of transport efficiency of placentas whose gestational age are among $(W-1, W+1)$ weeks. Again, Figure 12 indicates that transport efficiency is roughly an increasing function of gestational ages. Preterm newborns typically have less efficient placentas compared to infants born at term. This is consistent with the progressive development of vasculosyncytial membranes from the beginning of the third trimester.[5]

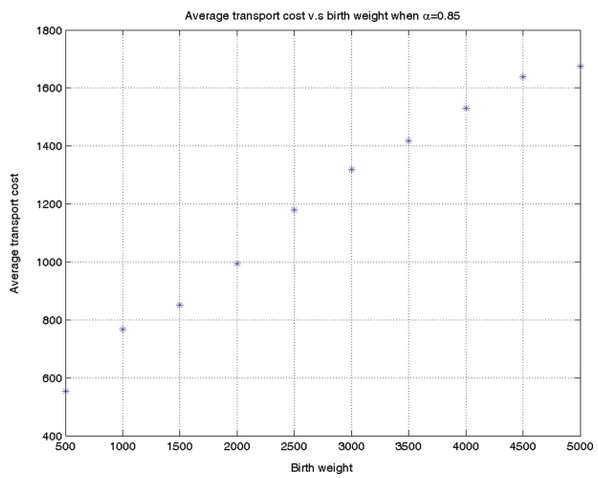

Fig. 9. Average transport cost C_α is nearly a linear function of birth weights.

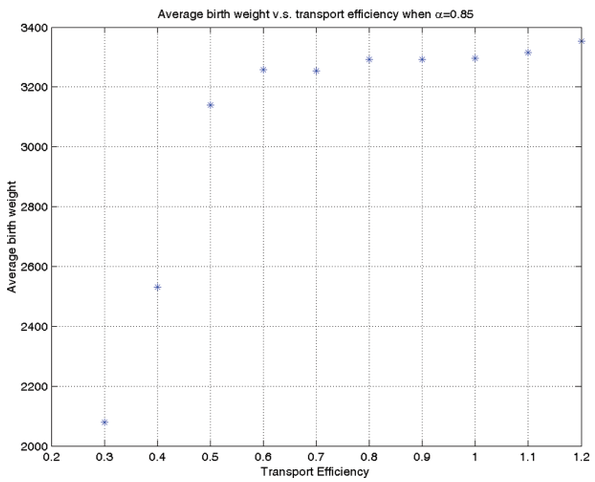

Fig. 11. Transport efficiency still has a positive relationship with averaged birth weights.

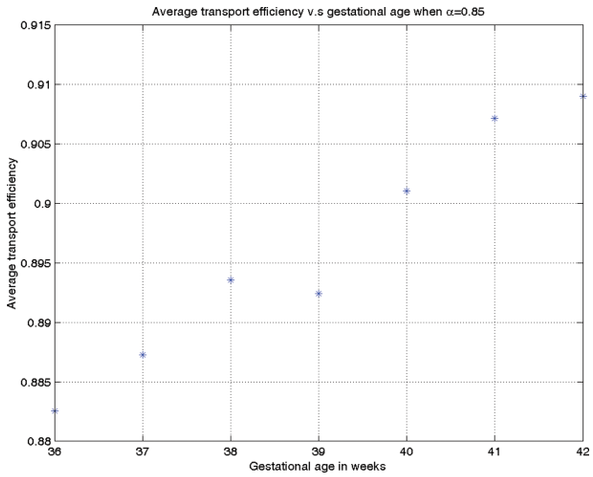

Fig. 12. Averaged transport efficiency has also a positive relationship with the gestational age.

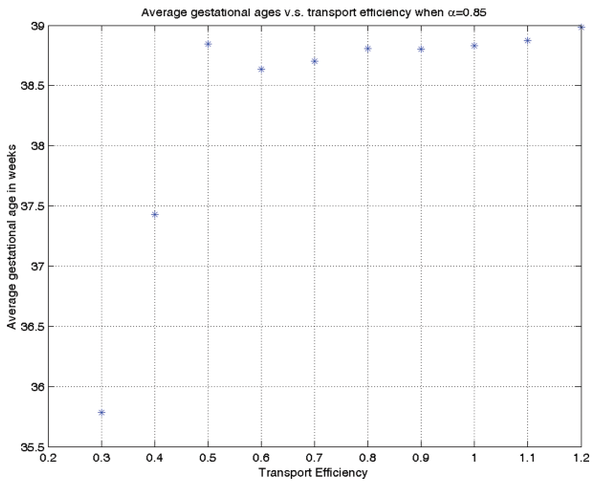

Fig. 13. Average gestational age is nearly an increasing and concave function of transport efficiency.

On the other hand, the correlation between placental transport efficiency and gestational age plateaus above a certain level of transport efficiency. In Figure 13, for each fixed transport efficiency E in $\{0.3, 0.4, \ldots, 1.2\}$, we calculate the average gestational age of newborns whose placentas have transport efficiency in the range of $(E - 0.2, E + 0.2)$. Average gestational age still increases as transport efficiency increases, but again with a decreased slop, indicating a smaller effect.

Summary

We have shown that placental efficiency as calculated from simple measures of perimeter and the distance of umbilical cord displacement from the center of the chorionic plate is correlated with birth weight and gestational age, and also that this relationship changes over gestational age and birth weight ranges consistent with what is well appreciated clinically.[8]

Moreover, the calculated transport efficiency demonstrates transitions that allow clear distinctions to be proposed between newborns exposed to an inefficient placenta (and hence to a compromised intrauterine environment) and those with adequate placental transport efficiency. Further studies will evaluate the multivariate contributions of gestational age and placental transport efficiency to birth weight.

Acknowledgments: The work of Q. Xia is supported by the NSF grant DMS-1109663. The work of C.M. Salafia is partially supported by the NIH grant R01-HD39373-01 and the SBIR grant 1 R43HD062307-01. Also, partial results of this article has been reported in the proceedings of the AMMCS conference in Ref. [14]. The authors appreciate helpful discussions with Dr. Simon Morgan.

References and Notes

1. M. Bernot, V. Caselles, and J. Morel; Traffic plans. Optimal Transportation Networks: Models and Theory; Series: Lecture Notes in Mathematics (2009), Vol. 1955.
2. A. Brancolini, G. Buttazzo, and F. Santambrogio; Path functions over Wasserstein spaces; *J. Eur. Math. Soc.* 8, 415 **(2006)**.
3. J. S. Gill, C. M. Salafia, D. Grebenkov, and D. D. Vvedensky; Modeling oxygen transport in human placental terminal villi; *J. Theor. Biol.* 21, 33 **(2011)**.
4. F. Maddalena, S. Solimini, and J. M. Morel; A variational model of irrigation patterns; *Interfaces and Free Boundaries* 5, 391 **(2003)**.
5. T. M. Mayhew; A stereological perspective on placental morphology in normal and complicated pregnancies; *J. Anat.* 215, 77 **(2009)**.
6. D. Misra, C. Salafia, A. Charles, and R. Miller; Birth weights smaller or larger than the placenta predict BMI and blood pressure at age 7 years; *J. Devel Origins Health Dis.* 1, 123 **(2010)**.
7. D. Misra, C. Salafia, A. Charles, and R. Miller; Placental measurements associated with IQ at age 7 years; *J. Devel Origins Health Dis.* 3, 190 **(2012)**.
8. R. A. Molteni; Placental growth and fetal/placental weight (F/P) ratios throughout gestation–their relationship to patterns of fetal growth; *Semin. Perinatol.* 8, 94 **(1984)**.
9. Q. Xia; Optimal paths related to transport problems; *Communications in Contemporary Mathematics* 5, 251 **(2003)**.
10. Q. Xia; The formation of tree leaf; *ESAIM Control Optim. Calc. Var.* 13, 359 **(2007)**.
11. Q. Xia; An application of optimal transport paths to urban transport networks; *Discrete and Continuous Dynmical Systems* 2005, 904 **(2005)**.
12. Q. Xia; Numerical simulation of optimal transport paths; *The Second International Conference on Computer Modeling and Simulation* **(2010)**, Vol. 1, pp. 521–525, arXiv:0807.3723.
13. Q. Xia and D. Unger; Diffusion-limited aggregation driven by optimal transportation; *Fractals* 18, 247 **(2010)**.
14. Q. Xia, C. M. Salafia, and S. Morgan; Optimal transport and placental function; *The proccedings of the AMMCS 2013 conference* held in Waterloo, Ontario, Canada, To appear.
15. M. Yampolskya, C. M. Salafia, O. Shlakhter, D. Haase, B. Euckerf, and J. Thorp; Modeling the variability of shapes of a human placenta; *Placenta* 29, 790 **(2008)**.
16. M. Yampolsky, C. M. Salafia, and O. Shlakhter; Probability distributions of placental morphological measurements and origins of variability of placental shapes; *Placenta* 34, 493 **(2013)**.

17. R. K. Seong, C. M. Salafia, and D. D. Vvedensky; Statistical topology of radial networks: A case study of tree leaves; *Philosophical Magazine* 1–16, iFirst **(2011)**.

18. R. K. Seong, P. Getreuer, Y. Li, T. Girardi, C. M. Salafia, and D. D. Vvedensky; Statistical geometry and topology of the human placenta; *Advances in Applied Mathematics, Modeling, and Computational Science Fields Institute Communications* 66, 187 **(2013)**.

19. A. Serov, D. Grebenkov, C. Salafia, and M. Filoche; A geometrical model for searching an optimal villi density in the inter-villous cross-sections of the human placenta; *Placenta* 34, A93 **(01/2013)**.

20. D. M. Thomas, N. Schwartz, K. Orzechowski, R. C. Miller, and C. M. Salafia; Parameter estimation and validation of a dynamic placental volume growth mode; *Reprod Sci.* 21, 386A **(2014)**.